

Search for Lepton Flavor Violation in the Decay $\tau^\pm \rightarrow \mu^\pm \gamma$

- B. Aubert,¹ R. Barate,¹ D. Boutigny,¹ F. Couderc,¹ Y. Karyotakis,¹ J. P. Lees,¹ V. Poireau,¹ V. Tisserand,¹ A. Zghiche,¹ E. Grauges-Pous,² A. Palano,³ A. Pompili,³ J. C. Chen,⁴ N. D. Qi,⁴ G. Rong,⁴ P. Wang,⁴ Y. S. Zhu,⁴ G. Eigen,⁵ I. Ofte,⁵ B. Stugu,⁵ G. S. Abrams,⁶ A. W. Borgland,⁶ A. B. Breon,⁶ D. N. Brown,⁶ J. Button-Shafer,⁶ R. N. Cahn,⁶ E. Charles,⁶ C. T. Day,⁶ M. S. Gill,⁶ A. V. Gritsan,⁶ Y. Groysman,⁶ R. G. Jacobsen,⁶ R. W. Kadel,⁶ J. Kadyk,⁶ L. T. Kerth,⁶ Yu. G. Kolomensky,⁶ G. Kukartsev,⁶ G. Lynch,⁶ L. M. Mir,⁶ P. J. Oddone,⁶ T. J. Orimoto,⁶ M. Pripstein,⁶ N. A. Roe,⁶ M. T. Ronan,⁶ W. A. Wenzel,⁶ M. Barrett,⁷ K. E. Ford,⁷ T. J. Harrison,⁷ A. J. Hart,⁷ C. M. Hawkes,⁷ S. E. Morgan,⁷ A. T. Watson,⁷ M. Fritsch,⁸ K. Goetzen,⁸ T. Held,⁸ H. Koch,⁸ B. Lewandowski,⁸ M. Pelizaeus,⁸ K. Peters,⁸ T. Schroeder,⁸ M. Steinke,⁸ J. T. Boyd,⁹ J. P. Burke,⁹ N. Chevalier,⁹ W. N. Cottingham,⁹ M. P. Kelly,⁹ T. E. Latham,⁹ F. F. Wilson,⁹ T. Cuhadar-Donszelmann,¹⁰ C. Hearty,¹⁰ N. S. Knecht,¹⁰ T. S. Mattison,¹⁰ J. A. McKenna,¹⁰ D. Thiessen,¹⁰ A. Khan,¹¹ P. Kyberd,¹¹ L. Teodorescu,¹¹ A. E. Blinov,¹² V. E. Blinov,¹² V. P. Druzhinin,¹² V. B. Golubev,¹² V. N. Ivanchenko,¹² E. A. Kravchenko,¹² A. P. Onuchin,¹² S. I. Serednyakov,¹² Yu. I. Skovpen,¹² E. P. Solodov,¹² A. N. Yushkov,¹² D. Best,¹³ M. Bruinsma,¹³ M. Chao,¹³ I. Eschrich,¹³ D. Kirkby,¹³ A. J. Lankford,¹³ M. Mandelkern,¹³ R. K. Mommsen,¹³ W. Roethel,¹³ D. P. Stoker,¹³ C. Buchanan,¹⁴ B. L. Hartfiel,¹⁴ A. J. R. Weinstein,¹⁴ S. D. Foulkes,¹⁵ J. W. Gary,¹⁵ O. Long,¹⁵ B. C. Shen,¹⁵ K. Wang,¹⁵ D. del Re,¹⁶ H. K. Hadavand,¹⁶ E. J. Hill,¹⁶ D. B. MacFarlane,¹⁶ H. P. Paar,¹⁶ Sh. Rahatlou,¹⁶ V. Sharma,¹⁶ J. W. Berryhill,¹⁷ C. Campagnari,¹⁷ A. Cunha,¹⁷ B. Dahmes,¹⁷ T. M. Hong,¹⁷ A. Lu,¹⁷ M. A. Mazur,¹⁷ J. D. Richman,¹⁷ W. Verkerke,¹⁷ T. W. Beck,¹⁸ A. M. Eisner,¹⁸ C. J. Flacco,¹⁸ C. A. Heusch,¹⁸ J. Kroeseberg,¹⁸ W. S. Lockman,¹⁸ G. Nesom,¹⁸ T. Schalk,¹⁸ B. A. Schumm,¹⁸ A. Seiden,¹⁸ P. Spradlin,¹⁸ D. C. Williams,¹⁸ M. G. Wilson,¹⁸ J. Albert,¹⁹ E. Chen,¹⁹ G. P. Dubois-Felsmann,¹⁹ A. Dvoretskii,¹⁹ D. G. Hitlin,¹⁹ I. Narsky,¹⁹ T. Piatenko,¹⁹ F. C. Porter,¹⁹ A. Ryd,¹⁹ A. Samuel,¹⁹ S. Yang,¹⁹ S. Jayatilleke,²⁰ G. Mancinelli,²⁰ B. T. Meadows,²⁰ M. D. Sokoloff,²⁰ F. Blanc,²¹ P. Bloom,²¹ S. Chen,²¹ W. T. Ford,²¹ U. Nauenberg,²¹ A. Olivas,²¹ P. Rankin,²¹ W. O. Ruddick,²¹ J. G. Smith,²¹ K. A. Ulmer,²¹ J. Zhang,²¹ L. Zhang,²¹ A. Chen,²² E. A. Eckhart,²² J. L. Harton,²² A. Soffer,²² W. H. Toki,²² R. J. Wilson,²² Q. Zeng,²² B. Spaan,²³ D. Altenburg,²⁴ T. Brandt,²⁴ J. Brose,²⁴ M. Dickopp,²⁴ E. Feltresi,²⁴ A. Hauke,²⁴ H. M. Lacker,²⁴ E. Maly,²⁴ R. Nogowski,²⁴ S. Otto,²⁴ A. Petzold,²⁴ G. Schott,²⁴ J. Schubert,²⁴ K. R. Schubert,²⁴ R. Schwierz,²⁴ J. E. Sundermann,²⁴ D. Bernard,²⁵ G. R. Bonneau,²⁵ P. Grenier,²⁵ S. Schrenk,²⁵ Ch. Thiebaux,²⁵ G. Vasileiadis,²⁵ M. Verderi,²⁵ D. J. Bard,²⁶ P. J. Clark,²⁶ F. Muheim,²⁶ S. Playfer,²⁶ Y. Xie,²⁶ M. Andreotti,²⁷ V. Azzolini,²⁷ D. Bettoni,²⁷ C. Bozzi,²⁷ R. Calabrese,²⁷ G. Cibinetto,²⁷ E. Luppi,²⁷ M. Negrini,²⁷ L. Piemontese,²⁷ A. Sarti,²⁷ F. Anulli,²⁸ R. Baldini-Ferroli,²⁸ A. Calcaterra,²⁸ R. de Sangro,²⁸ G. Finocchiaro,²⁸ P. Patteri,²⁸ I. M. Peruzzi,²⁸ M. Piccolo,²⁸ A. Zallo,²⁸ A. Buzzo,²⁹ R. Capra,²⁹ R. Contri,²⁹ G. Crosetti,²⁹ M. Lo Vetere,²⁹ M. Macri,²⁹ M. R. Monge,²⁹ S. Passaggio,²⁹ C. Patrignani,²⁹ E. Robutti,²⁹ A. Santroni,²⁹ S. Tosi,²⁹ S. Bailey,³⁰ G. Brandenburg,³⁰ K. S. Chaisanguanthum,³⁰ M. Morii,³⁰ E. Won,³⁰ R. S. Dubitzky,³¹ U. Langenegger,³¹ J. Marks,³¹ U. Uwer,³¹ W. Bhimji,³² D. A. Bowerman,³² P. D. Dauncey,³² U. Egede,³² J. R. Gaillard,³² G. W. Morton,³² J. A. Nash,³² M. B. Nikolich,³² G. P. Taylor,³² M. J. Charles,³³ G. J. Grenier,³³ U. Mallik,³³ A. K. Mohapatra,³³ J. Cochran,³⁴ H. B. Crawley,³⁴ J. Lamsa,³⁴ W. T. Meyer,³⁴ S. Prell,³⁴ E. I. Rosenberg,³⁴ A. E. Rubin,³⁴ J. Yi,³⁴ N. Arnaud,³⁵ M. Davier,³⁵ X. Giroux,³⁵ G. Grosdidier,³⁵ A. Höcker,³⁵ F. Le Diberder,³⁵ V. Lepeltier,³⁵ A. M. Lutz,³⁵ T. C. Petersen,³⁵ M. Pierini,³⁵ S. Plaszczynski,³⁵ M. H. Schune,³⁵ G. Wormser,³⁵ C. H. Cheng,³⁶ D. J. Lange,³⁶ M. C. Simani,³⁶ D. M. Wright,³⁶ A. J. Bevan,³⁷ C. A. Chavez,³⁷ J. P. Coleman,³⁷ I. J. Forster,³⁷ J. R. Fry,³⁷ E. Gabathuler,³⁷ R. Gamet,³⁷ D. E. Hutchcroft,³⁷ R. J. Parry,³⁷ D. J. Payne,³⁷ C. Touramanis,³⁷ C. M. Cormack,³⁸ F. Di Lodovico,³⁸ C. L. Brown,³⁹ G. Cowan,³⁹ R. L. Flack,³⁹ H. U. Flaecher,³⁹ M. G. Green,³⁹ P. S. Jackson,³⁹ T. R. McMahon,³⁹ S. Ricciardi,³⁹ F. Salvatore,³⁹ M. A. Winter,³⁹ D. Brown,⁴⁰ C. L. Davis,⁴⁰ J. Allison,⁴¹ N. R. Barlow,⁴¹ R. J. Barlow,⁴¹ M. C. Hodgkinson,⁴¹ G. D. Lafferty,⁴¹ M. T. Naisbit,⁴¹ J. C. Williams,⁴¹ C. Chen,⁴² A. Farbin,⁴² W. D. Hulsbergen,⁴² A. Jawahery,⁴² D. Kovalskyi,⁴² C. K. Lae,⁴² V. Lillard,⁴² D. A. Roberts,⁴² G. Blaylock,⁴³ C. Dallapiccola,⁴³ S. S. Hertzbach,⁴³ R. Kofler,⁴³

V. B. Koptchev,⁴³ T. B. Moore,⁴³ S. Saremi,⁴³ H. Staengle,⁴³ S. Willocq,⁴³ R. Cowan,⁴⁴ K. Koenike,⁴⁴ G. Sciolla,⁴⁴ S. J. Sekula,⁴⁴ F. Taylor,⁴⁴ R. K. Yamamoto,⁴⁴ P. M. Patel,⁴⁵ S. H. Robertson,⁴⁵ A. Lazzaro,⁴⁶ V. Lombardo,⁴⁶ F. Palombo,⁴⁶ J. M. Bauer,⁴⁷ L. Cremaldi,⁴⁷ V. Eschenburg,⁴⁷ R. Godang,⁴⁷ R. Kroeger,⁴⁷ J. Reidy,⁴⁷ D. A. Sanders,⁴⁷ D. J. Summers,⁴⁷ H. W. Zhao,⁴⁷ S. Brunet,⁴⁸ D. Côté,⁴⁸ P. Taras,⁴⁸ H. Nicholson,⁴⁹ N. Cavallo,^{50,*} F. Fabozzi,^{50,*} C. Gatto,⁵⁰ L. Lista,⁵⁰ D. Monorchio,⁵⁰ P. Paolucci,⁵⁰ D. Piccolo,⁵⁰ C. Sciacca,⁵⁰ M. Baak,⁵¹ H. Bulten,⁵¹ G. Raven,⁵¹ H. L. Snoek,⁵¹ L. Wilden,⁵¹ C. P. Jessop,⁵² J. M. LoSecco,⁵² T. Allmendinger,⁵³ G. Benelli,⁵³ K. K. Gan,⁵³ K. Honscheid,⁵³ D. Hufnagel,⁵³ H. Kagan,⁵³ R. Kass,⁵³ T. Pulliam,⁵³ A. M. Rahimi,⁵³ R. Ter-Antonyan,⁵³ Q. K. Wong,⁵³ J. Brau,⁵⁴ R. Frey,⁵⁴ O. Igonkina,⁵⁴ M. Lu,⁵⁴ C. T. Potter,⁵⁴ N. B. Sinev,⁵⁴ D. Strom,⁵⁴ E. Torrence,⁵⁴ F. Colecchia,⁵⁵ A. Dorigo,⁵⁵ F. Galeazzi,⁵⁵ M. Margoni,⁵⁵ M. Morandin,⁵⁵ M. Posocco,⁵⁵ M. Rotondo,⁵⁵ F. Simonetto,⁵⁵ R. Stroili,⁵⁵ C. Voci,⁵⁵ M. Benayoun,⁵⁶ H. Briand,⁵⁶ J. Chauveau,⁵⁶ P. David,⁵⁶ L. Del Buono,⁵⁶ Ch. de la Vaissière,⁵⁶ O. Hamon,⁵⁶ M. J. J. John,⁵⁶ Ph. Leruste,⁵⁶ J. Malclès,⁵⁶ J. Ocariz,⁵⁶ L. Roos,⁵⁶ G. Therin,⁵⁶ P. K. Behera,⁵⁷ L. Gladney,⁵⁷ Q. H. Guo,⁵⁷ J. Panetta,⁵⁷ M. Biasini,⁵⁸ R. Covarelli,⁵⁸ M. Pioppi,⁵⁸ C. Angelini,⁵⁹ G. Batignani,⁵⁹ S. Bettarini,⁵⁹ M. Bondioli,⁵⁹ F. Bucci,⁵⁹ G. Calderini,⁵⁹ M. Carpinelli,⁵⁹ F. Forti,⁵⁹ M. A. Giorgi,⁵⁹ A. Lusiani,⁵⁹ G. Marchiori,⁵⁹ M. Morganti,⁵⁹ N. Neri,⁵⁹ E. Paoloni,⁵⁹ M. Rama,⁵⁹ G. Rizzo,⁵⁹ G. Simi,⁵⁹ J. Walsh,⁵⁹ M. Haire,⁶⁰ D. Judd,⁶⁰ K. Paick,⁶⁰ D. E. Wagoner,⁶⁰ N. Danielson,⁶¹ P. Elmer,⁶¹ Y. P. Lau,⁶¹ C. Lu,⁶¹ V. Miftakov,⁶¹ J. Olsen,⁶¹ A. J. S. Smith,⁶¹ A. V. Telnov,⁶¹ F. Bellini,⁶² G. Cavoto,^{61,62} A. D'Orazio,⁶² E. Di Marco,⁶² R. Faccini,⁶² F. Ferrarotto,⁶² F. Ferroni,⁶² M. Gaspero,⁶² L. Li Gioi,⁶² M. A. Mazzoni,⁶² S. Morganti,⁶² G. Piredda,⁶² F. Polci,⁶² F. Safai Tehrani,⁶² C. Voena,⁶² S. Christ,⁶³ H. Schröder,⁶³ G. Wagner,⁶³ R. Waldi,⁶³ T. Adye,⁶⁴ N. De Groot,⁶⁴ B. Franek,⁶⁴ G. P. Gopal,⁶⁴ E. O. Olaiya,⁶⁴ R. Aleksan,⁶⁵ S. Emery,⁶⁵ A. Gaidot,⁶⁵ S. F. Ganzhur,⁶⁵ P.-F. Giraud,⁶⁵ G. Graziani,⁶⁵ G. Hamel de Monchenault,⁶⁵ W. Kozanecki,⁶⁵ M. Legendre,⁶⁵ G. W. London,⁶⁵ B. Mayer,⁶⁵ G. Vasseur,⁶⁵ Ch. Yèche,⁶⁵ M. Zito,⁶⁵ M. V. Purohit,⁶⁶ A. W. Weidemann,⁶⁶ J. R. Wilson,⁶⁶ F. X. Yumiceva,⁶⁶ T. Abe,⁶⁷ D. Aston,⁶⁷ R. Bartoldus,⁶⁷ N. Berger,⁶⁷ A. M. Boyarski,⁶⁷ O. L. Buchmueller,⁶⁷ R. Claus,⁶⁷ M. R. Convery,⁶⁷ M. Cristinziani,⁶⁷ G. De Nardo,⁶⁷ J. C. Dingfelder,⁶⁷ D. Dong,⁶⁷ J. Dorfan,⁶⁷ D. Dujmic,⁶⁷ W. Dunwoodie,⁶⁷ S. Fan,⁶⁷ R. C. Field,⁶⁷ T. Glanzman,⁶⁷ S. J. Gowdy,⁶⁷ T. Hadig,⁶⁷ V. Halyo,⁶⁷ C. Hast,⁶⁷ T. Hryna'ova,⁶⁷ W. R. Innes,⁶⁷ M. H. Kelsey,⁶⁷ P. Kim,⁶⁷ M. L. Kocian,⁶⁷ D. W. G. S. Leith,⁶⁷ J. Libby,⁶⁷ S. Luitz,⁶⁷ V. Luth,⁶⁷ H. L. Lynch,⁶⁷ H. Marsiske,⁶⁷ R. Messner,⁶⁷ D. R. Muller,⁶⁷ C. P. O'Grady,⁶⁷ V. E. Ozcan,⁶⁷ A. Perazzo,⁶⁷ M. Perl,⁶⁷ B. N. Ratcliff,⁶⁷ A. Roodman,⁶⁷ A. A. Salnikov,⁶⁷ R. H. Schindler,⁶⁷ J. Schwiening,⁶⁷ A. Snyder,⁶⁷ A. Soha,⁶⁷ J. Stelzer,⁶⁷ J. Strube,^{54,67} D. Su,⁶⁷ M. K. Sullivan,⁶⁷ J. Va'vra,⁶⁷ S. R. Wagner,⁶⁷ M. Weaver,⁶⁷ W. J. Wisniewski,⁶⁷ M. Wittgen,⁶⁷ D. H. Wright,⁶⁷ A. K. Yarritu,⁶⁷ C. C. Young,⁶⁷ P. R. Burchat,⁶⁸ A. J. Edwards,⁶⁸ S. A. Majewski,⁶⁸ B. A. Petersen,⁶⁸ C. Roat,⁶⁸ M. Ahmed,⁶⁹ S. Ahmed,⁶⁹ M. S. Alam,⁶⁹ J. A. Ernst,⁶⁹ M. A. Saeed,⁶⁹ M. Saleem,⁶⁹ F. R. Wappler,⁶⁹ W. Bugg,⁷⁰ M. Krishnamurthy,⁷⁰ S. M. Spanier,⁷⁰ R. Eckmann,⁷¹ H. Kim,⁷¹ J. L. Ritchie,⁷¹ A. Satpathy,⁷¹ R. F. Schwitters,⁷¹ J. M. Izen,⁷² I. Kitayama,⁷² X. C. Lou,⁷² S. Ye,⁷² F. Bianchi,⁷³ M. Bona,⁷³ F. Gallo,⁷³ D. Gamba,⁷³ L. Bosisio,⁷⁴ C. Cartaro,⁷⁴ F. Cossutti,⁷⁴ G. Della Ricca,⁷⁴ S. Dittongo,⁷⁴ S. Grancagnolo,⁷⁴ L. Lanceri,⁷⁴ P. Poropat,^{74,†} L. Vitale,⁷⁴ G. Vuagnin,⁷⁴ F. Martinez-Vidal,^{2,75} R. S. Panvini,^{76,†} Sw. Banerjee,⁷⁷ B. Bhuyan,⁷⁷ C. M. Brown,⁷⁷ D. Fortin,⁷⁷ K. Hamano,⁷⁷ P. D. Jackson,⁷⁷ R. Kowalewski,⁷⁷ J. M. Roney,⁷⁷ R. J. Sobie,⁷⁷ Z. Yun,⁷⁷ J. J. Back,⁷⁸ P. F. Harrison,⁷⁸ G. B. Mohanty,⁷⁸ H. R. Band,⁷⁹ X. Chen,⁷⁹ B. Cheng,⁷⁹ S. Dasu,⁷⁹ M. Datta,⁷⁹ A. M. Eichenbaum,⁷⁹ K. T. Flood,⁷⁹ M. Graham,⁷⁹ J. J. Hollar,⁷⁹ J. R. Johnson,⁷⁹ P. E. Kutter,⁷⁹ H. Li,⁷⁹ R. Liu,⁷⁹ A. Mihalyi,⁷⁹ Y. Pan,⁷⁹ R. Prepost,⁷⁹ P. Tan,⁷⁹ J. H. von Wimmersperg-Toeller,⁷⁹ J. Wu,⁷⁹ S. L. Wu,⁷⁹ Z. Yu,⁷⁹ M. G. Greene,⁸⁰ and H. Neal⁸⁰

(The BABAR Collaboration)

¹Laboratoire de Physique des Particules, F-74941 Annecy-le-Vieux, France

²IFAE, Universitat Autònoma de Barcelona, E-08193 Bellaterra, Barcelona, Spain

³Università di Bari, Dipartimento di Fisica and INFN, I-70126 Bari, Italy

⁴Institute of High Energy Physics, Beijing 100039, China

⁵University of Bergen, Inst. of Physics, N-5007 Bergen, Norway

⁶Lawrence Berkeley National Laboratory and University of California, Berkeley, California 94720, USA

⁷University of Birmingham, Birmingham, B15 2TT, United Kingdom

⁸Ruhr Universität Bochum, Institut für Experimentalphysik 1, D-44780 Bochum, Germany

⁹University of Bristol, Bristol BS8 1TL, United Kingdom

¹⁰University of British Columbia, Vancouver, British Columbia, Canada V6T 1Z1

¹¹Brunel University, Uxbridge, Middlesex UB8 3PH, United Kingdom

¹²Budker Institute of Nuclear Physics, Novosibirsk 630090, Russia

¹³University of California at Irvine, Irvine, California 92697, USA

- ¹⁴University of California at Los Angeles, Los Angeles, California 90024, USA
¹⁵University of California at Riverside, Riverside, California 92521, USA
¹⁶University of California at San Diego, La Jolla, California 92093, USA
¹⁷University of California at Santa Barbara, Santa Barbara, California 93106, USA
¹⁸University of California at Santa Cruz, Institute for Particle Physics, Santa Cruz, California 95064, USA
¹⁹California Institute of Technology, Pasadena, California 91125, USA
²⁰University of Cincinnati, Cincinnati, Ohio 45221, USA
²¹University of Colorado, Boulder, Colorado 80309, USA
²²Colorado State University, Fort Collins, Colorado 80523, USA
²³Universität Dortmund, Institut für Physik, D-44221 Dortmund, Germany
²⁴Technische Universität Dresden, Institut für Kern- und Teilchenphysik, D-01062 Dresden, Germany
²⁵Ecole Polytechnique, LLR, F-91128 Palaiseau, France
²⁶University of Edinburgh, Edinburgh EH9 3JZ, United Kingdom
²⁷Università di Ferrara, Dipartimento di Fisica and INFN, I-44100 Ferrara, Italy
²⁸Laboratori Nazionali di Frascati dell'INFN, I-00044 Frascati, Italy
²⁹Università di Genova, Dipartimento di Fisica and INFN, I-16146 Genova, Italy
³⁰Harvard University, Cambridge, Massachusetts 02138, USA
³¹Universität Heidelberg, Physikalisches Institut, Philosophenweg 12, D-69120 Heidelberg, Germany
³²Imperial College London, London, SW7 2AZ, United Kingdom
³³University of Iowa, Iowa City, Iowa 52242, USA
³⁴Iowa State University, Ames, Iowa 50011-3160, USA
³⁵Laboratoire de l'Accélérateur Linéaire, F-91898 Orsay, France
³⁶Lawrence Livermore National Laboratory, Livermore, California 94550, USA
³⁷University of Liverpool, Liverpool L69 7ZE, United Kingdom
³⁸Queen Mary, University of London, E1 4NS, United Kingdom
³⁹University of London, Royal Holloway and Bedford New College, Egham, Surrey TW20 0EX, United Kingdom
⁴⁰University of Louisville, Louisville, Kentucky 40292, USA
⁴¹University of Manchester, Manchester M13 9PL, United Kingdom
⁴²University of Maryland, College Park, Maryland 20742, USA
⁴³University of Massachusetts, Amherst, Massachusetts 01003, USA
⁴⁴Massachusetts Institute of Technology, Laboratory for Nuclear Science, Cambridge, Massachusetts 02139, USA
⁴⁵McGill University, Montréal, Quebec, Canada H3A 2T8
⁴⁶Università di Milano, Dipartimento di Fisica and INFN, I-20133 Milano, Italy
⁴⁷University of Mississippi, University, Mississippi 38677, USA
⁴⁸Université de Montréal, Laboratoire René J. A. Lévesque, Montréal, Quebec, Canada H3C 3J7
⁴⁹Mount Holyoke College, South Hadley, Massachusetts 01075, USA
⁵⁰Università di Napoli Federico II, Dipartimento di Scienze Fisiche and INFN, I-80126, Napoli, Italy
⁵¹NIKHEF, National Institute for Nuclear Physics and High Energy Physics, NL-1009 DB Amsterdam, The Netherlands
⁵²University of Notre Dame, Notre Dame, Indiana 46556, USA
⁵³Ohio State University, Columbus, Ohio 43210, USA
⁵⁴University of Oregon, Eugene, Oregon 97403, USA
⁵⁵Università di Padova, Dipartimento di Fisica and INFN, I-35131 Padova, Italy
⁵⁶Universités Paris VI et VII, Laboratoire de Physique Nucléaire et de Hautes Energies, F-75252 Paris, France
⁵⁷University of Pennsylvania, Philadelphia, Pennsylvania 19104, USA
⁵⁸Università di Perugia, Dipartimento di Fisica and INFN, I-06100 Perugia, Italy
⁵⁹Università di Pisa, Dipartimento di Fisica, Scuola Normale Superiore and INFN, I-56127 Pisa, Italy
⁶⁰Prairie View A&M University, Prairie View, Texas 77446, USA
⁶¹Princeton University, Princeton, New Jersey 08544, USA
⁶²Università di Roma La Sapienza, Dipartimento di Fisica and INFN, I-00185 Roma, Italy
⁶³Universität Rostock, D-18051 Rostock, Germany
⁶⁴Rutherford Appleton Laboratory, Chilton, Didcot, Oxon, OX11 0QX, United Kingdom
⁶⁵DSM/Dapnia, CEA/Saclay, F-91191 Gif-sur-Yvette, France
⁶⁶University of South Carolina, Columbia, South Carolina 29208, USA
⁶⁷Stanford Linear Accelerator Center, Stanford, California 94309, USA
⁶⁸Stanford University, Stanford, California 94305-4060, USA
⁶⁹State University of New York, Albany, New York 12222, USA
⁷⁰University of Tennessee, Knoxville, Tennessee 37996, USA
⁷¹University of Texas at Austin, Austin, Texas 78712, USA
⁷²University of Texas at Dallas, Richardson, Texas 75083, USA
⁷³Università di Torino, Dipartimento di Fisica Sperimentale and INFN, I-10125 Torino, Italy
⁷⁴Università di Trieste, Dipartimento di Fisica and INFN, I-34127 Trieste, Italy
⁷⁵IFIC, Universitat de Valencia-CSIC, E-46071 Valencia, Spain
⁷⁶Vanderbilt University, Nashville, Tennessee 37235, USA
⁷⁷University of Victoria, Victoria, British Columbia, Canada V8W 3P6

⁷⁸Department of Physics, University of Warwick, Coventry CV4 7AL, United Kingdom

⁷⁹University of Wisconsin, Madison, Wisconsin 53706, USA

⁸⁰Yale University, New Haven, Connecticut 06511, USA

(Dated: June 21, 2021)

A search for the nonconservation of lepton flavor number in the decay $\tau^\pm \rightarrow \mu^\pm \gamma$ has been performed using $2.07 \times 10^8 e^+e^- \rightarrow \tau^+\tau^-$ events produced at a center-of-mass energy near 10.58 GeV with the *BABAR* detector at the PEP-II storage ring. We find no evidence for a signal and set an upper limit on the branching ratio of $\mathcal{B}(\tau^\pm \rightarrow \mu^\pm \gamma) < 6.8 \times 10^{-8}$ at 90% confidence level.

PACS numbers: 13.35.Dx, 14.60.Fg, 11.30.Hv

Decays violating lepton flavor number, if observed, would be among the most theoretically clean signatures of new physics and the decay $\tau^\pm \rightarrow \mu^\pm \gamma$ is one such process. It is expected with rates as high as several parts per million in some supersymmetric models [1, 2], despite the stringent experimental limit on the related $\mu^\pm \rightarrow e^\pm \gamma$ decay [3]. In a modest extension to the Standard Model (SM) incorporating finite ν masses [4], the branching ratio is many orders of magnitude below experimental accessibility [5], and so an observation of this mode would unambiguously indicate new physics. Currently the most stringent limit is $\mathcal{B}(\tau^\pm \rightarrow \mu^\pm \gamma) < 3.1 \times 10^{-7}$ at 90% confidence level (c.l.) from the *BELLE* experiment [6].

The search for $\tau^\pm \rightarrow \mu^\pm \gamma$ decays reported here uses data recorded by the *BABAR* detector at the SLAC PEP-II asymmetric-energy e^+e^- storage ring. The data sample consists of an integrated luminosity of $L = 210.6 \text{ fb}^{-1}$ recorded at a center-of-mass energy (\sqrt{s}) of $\sqrt{s} = 10.58 \text{ GeV}$, and 21.6 fb^{-1} recorded at $\sqrt{s} = 10.54 \text{ GeV}$. The luminosity-weighted average cross section for $e^+e^- \rightarrow \tau^+\tau^-$ is $\sigma_{\tau\tau} = (0.89 \pm 0.02) \text{ nb}$ [7], corresponding to a data sample of $2.07 \times 10^8 \tau$ -pair events.

The *BABAR* detector is described in detail in Ref. [8]. Charged particles are reconstructed as tracks with a 5-layer silicon vertex tracker and a 40-layer drift chamber (DCH) inside a 1.5-T solenoidal magnet. An electromagnetic calorimeter (EMC) consisting of 6580 CsI(Tl) crystals is used to identify electrons and photons. The flux return of the solenoid, instrumented with resistive plate chambers (IFR), is used to identify muons.

The signature of the signal process is the presence of an isolated μ and γ having an invariant mass consistent with that of the τ ($1.777 \text{ GeV}/c^2$ [9]) and a total energy ($E_{\mu\gamma}$) equal to $\sqrt{s}/2$ in the event center-of-mass (c.m.) frame, and properties of the other particles in the event which are consistent with a SM τ decay. Such events are simulated with higher-order radiative corrections using the **KK2f** Monte Carlo (MC) generator [7] where one τ decays into $\mu\gamma$ according to phase space [10], while the other τ decays according to measured rates [11] simulated with **Tauola** [12, 13]. The detector response is simulated with **GEANT4** [14]. The simulated events for signal as well as SM background processes [7, 12, 13, 15, 16] are then reconstructed in the same manner as data. The MC backgrounds are used for selection optimization and

efficiency systematic studies, but not for the final background estimation, which relies solely on data.

Events with two or four well reconstructed tracks and zero net charge are selected. The magnitude of the thrust vector calculated with all observed charged and neutral particles, characterising the direction of maximum energy flow in the event [17], is required to lie between 0.900 and 0.975 to suppress $e^+e^- \rightarrow q\bar{q}$ backgrounds with low thrust and $e^+e^- \rightarrow \mu^+\mu^-$ and Bhabha backgrounds with thrust close to unity. Other non- τ backgrounds are suppressed by requiring the polar angle (θ_{miss}) of the missing momentum associated with the neutrinos in the event to lie within the detector acceptance ($-0.76 < \cos \theta_{miss} < 0.92$), and the scaled missing c.m. transverse momentum relative to the beam axis (p_{miss}^T/\sqrt{s}) to be greater than 0.068 (0.009) for events with two (four) tracks.

The signal-side hemisphere, defined with respect to the thrust axis, is required to contain one track with c.m. momentum less than $4.5 \text{ GeV}/c$ and at least one γ with a c.m. energy greater than 200 MeV. The track must be identified as a μ using DCH, EMC and IFR information and the γ candidate is the one which gives the mass of the $\mu\gamma$ system closest to the τ mass. This provides the correct pairing for 99.9% of selected signal events. The resolution of the $\mu\gamma$ mass is improved by assigning the point of closest approach of the μ track to the e^+e^- collision axis as the origin of the γ candidate and by using a kinematic fit with $E_{\mu\gamma}$ constrained to $\sqrt{s}/2$. This energy-constrained mass (m_{EC}) and $\Delta E = E_{\mu\gamma} - \sqrt{s}/2$ are independent variables apart from small correlations arising from initial and final state radiation. The mean and standard deviation of the m_{EC} and ΔE distributions for reconstructed MC signal events are: $\langle m_{EC} \rangle = 1777 \text{ MeV}/c^2$, $\sigma(m_{EC}) = 9 \text{ MeV}/c^2$, $\langle \Delta E \rangle = -9 \text{ MeV}$, $\sigma(\Delta E) = 45 \text{ MeV}$, where the shift in $\langle \Delta E \rangle$ comes from photon energy reconstruction effects. We blind the data events within a 3σ ellipse centered on $\langle m_{EC} \rangle$ and $\langle \Delta E \rangle$ until completing all optimization and systematic studies of the selection criteria.

The dominant backgrounds are from $e^+e^- \rightarrow \mu^+\mu^-$ and $e^+e^- \rightarrow \tau^+\tau^-$ (with a $\tau^\pm \rightarrow \mu^\pm \nu\bar{\nu}$ decay) events with an energetic γ from initial or final state radiation or in the τ decay. For these backgrounds, the γ is predominantly along the μ flight direction; thus we require $|\cos \theta_H| < 0.8$, where θ_H is the angle between the μ

momentum in the reconstructed τ rest frame and the τ momentum in the laboratory frame. Backgrounds arising from $\tau^\pm \rightarrow h^\pm (\geq 1)\pi^0\nu$ decays with the hadronic track (h) mis-identified as a μ , are reduced by requiring the total c.m. energy of non-signal γ candidates in the signal-side hemisphere to be less than 200 MeV. If the reconstructed neutral candidate identified as the signal γ , has at least 1% likelihood of arising from overlapping daughters in $\pi^0 \rightarrow \gamma\gamma$ decays, then the event is rejected.

The tag-side hemisphere, which is expected to contain a SM τ decay, is required to have a total invariant mass less than $1.6 \text{ GeV}/c^2$ and a c.m. momentum for each track less than $4.0 \text{ GeV}/c$ to reduce background from $e^+e^- \rightarrow q\bar{q}$ and $e^+e^- \rightarrow \mu^+\mu^-$ processes, respectively. The $q\bar{q}$ background is further reduced by requiring the hemisphere to have no more than six γ candidates.

A tag-side hemisphere containing a single track is classified as e-tag, μ -tag or h-tag if the total photon c.m. energy in the hemisphere is no more than 200 MeV and the track is exclusively identified as an electron (e-tag), as a muon (μ -tag) or as neither (h-tag). If the total photon c.m. energy in the hemisphere is more than 200 MeV, then events are selected if the track is exclusively identified as an electron (ey-tag) or as neither an electron nor as a muon (h γ -tag). These allow for the presence of radiation in $\tau^\pm \rightarrow e^\pm\nu\bar{\nu}$ decays and for photons from $\pi^0 \rightarrow \gamma\gamma$ in $\tau^\pm \rightarrow h^\pm (\geq 1)\pi^0\nu$ decays. If the tag-side contains three tracks, the event is classified as a 3h-tag. We explored other tag-side channels but the sensitivity of the search does not improve by including them.

Hadronic τ decays have only one missing ν , a feature used to purify the sample. Taking the tag-side τ direction to be opposite the fitted signal $\mu\gamma$ candidate, we use all tracks and γ candidates on the tag-side to calculate the invariant mass squared of the missing ν (m_ν^2), and require $|m_\nu^2|$ to be less than $0.4 \text{ GeV}^2/c^4$ for h-tag and 3h-tag events and less than $0.8 \text{ GeV}^2/c^4$ for h γ -tag events.

At this stage of the analysis, 15% of the MC signal events survive within a Grand Side Band (GSB) region defined as: $m_{\text{EC}} \in [1.5, 2.1] \text{ GeV}/c^2$, $\Delta E \in [-1.0, 0.5] \text{ GeV}$. The non-blinded part of the GSB contains 4688 data events, which agrees with the MC background expectation of 4924 events to within 5%. Out of these MC events, 80% are from $e^+e^- \rightarrow \tau^+\tau^-$, 82% of which are $\tau^\pm \rightarrow \mu^\pm\nu\bar{\nu}$ decays on the signal-side.

To further suppress the backgrounds, separate neural net (NN) based discriminators are used for each of the six tags. Five observables serve as input to the NN: the missing mass of the event, the highest c.m. momentum of the tag-side track(s), $\cos\theta_H$, p_{miss}^T and m_ν^2 . Each NN is trained using data in the non-blinded part of the GSB to describe the background and $\mu\gamma$ MC in the full GSB region to describe the signal. The NN output distributions of the data (Figure 1) are in good agreement with MC backgrounds both in shape and absolute rates, as are the input observables. The MC signal within a

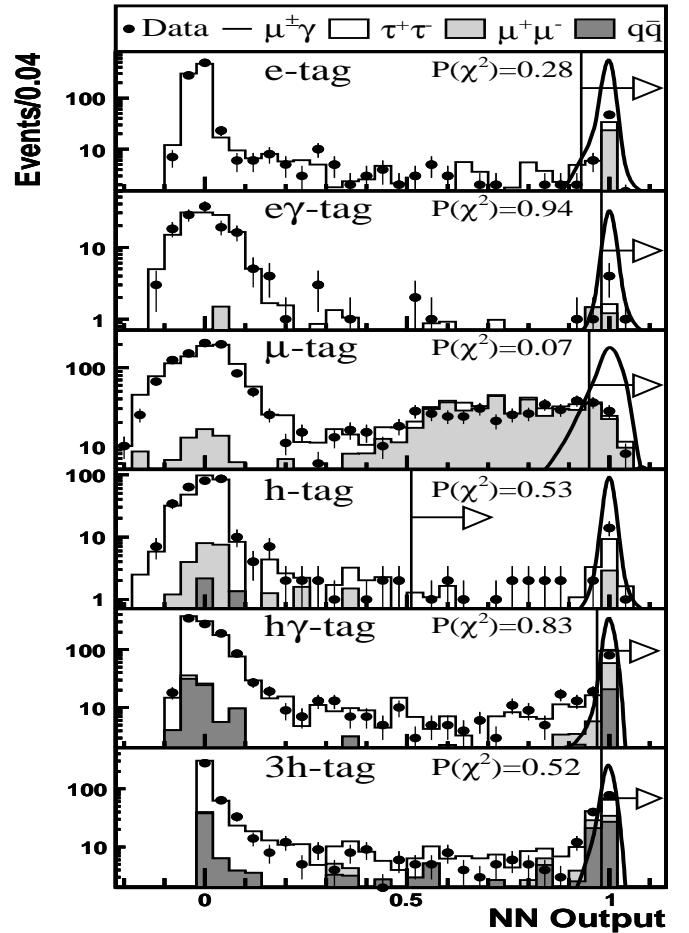


FIG. 1: NN output shown for data (dots), MC backgrounds (histograms normalized to the luminosity) and MC signal (curves with arbitrary normalization) in the GSB region. Lines with arrows indicate optimized cut positions. The probability of the data-MC χ^2 is indicated for each tag mode.

2σ ellipse in the $m_{\text{EC}}-\Delta E$ plane centered on $\langle m_{\text{EC}} \rangle$ and $\langle \Delta E \rangle$, and the MC background interpolated from m_{EC} sidebands ($|m_{\text{EC}} - \langle m_{\text{EC}} \rangle| > 3\sigma$ within the GSB and $|\Delta E - \langle \Delta E \rangle| < 3\sigma$) are then used to optimize the cut value on the NN output based on the expected 90% c.l. upper limit. The optimized NN cut values are restricted to be > 0.5 . Within the $\pm 3\sigma$ band in ΔE , the MC predicts that 66% of the selected background comes from $e^+e^- \rightarrow \mu^+\mu^-$, 27% from $e^+e^- \rightarrow \tau^+\tau^-$ and the rest from $e^+e^- \rightarrow q\bar{q}$ processes.

With the data unblinded, we find four events in the 2σ signal ellipse where we expect 6.2 ± 0.5 events, obtained from a linear interpolation of the data in the m_{EC} sidebands. Other polynomials up to at least fifth order predict the same level of background to within half a standard deviation. The agreement between observed data and background expectations across the different tagging modes are shown in Table I.

The relative systematic uncertainties on the trigger

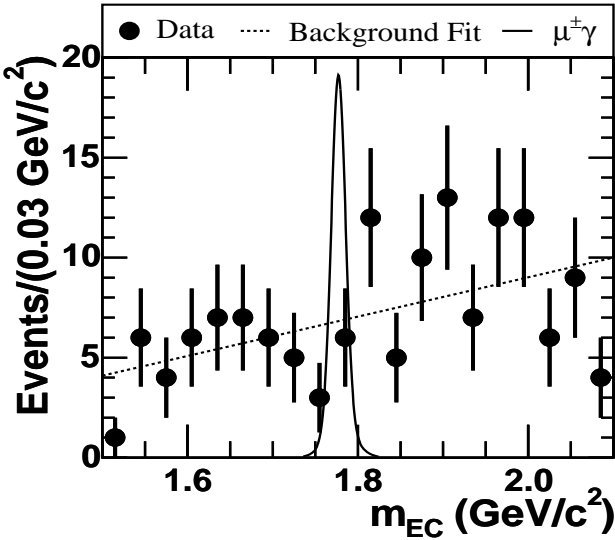


FIG. 2: m_{EC} distribution of data (dots), the background component of the fit (dotted line) and MC signal (curve with arbitrary normalization) for $|\Delta E - \langle \Delta E \rangle| < 2\sigma$. The χ^2 between data and the background component is 16.0 for 20 bins.

	Tag:	e	$e\gamma$	μ	h	$h\gamma$	3h	all
GSB	Data	57	6	67	31	92	78	331
	MC	46.4	2.7	63.1	19.2	108.9	64.9	305
	$\varepsilon(\%)$	1.88	0.27	1.80	1.44	3.72	1.85	11.0
2σ signal ellipse	Selected	1	0	1	0	1	1	4
	Expected	1.1	0.1	1.9	0.5	1.8	0.9	6.2
	from Data	± 0.2	± 0.1	± 0.3	± 0.1	± 0.3	± 0.2	± 0.5
	$\varepsilon(\%)$	1.27	0.18	1.31	0.89	2.56	1.22	7.42
$\pm 2\sigma$ in ΔE	Data	20	0	51	9	41	20	141
	$\varepsilon(\%)$	1.62	0.23	1.63	1.13	3.22	1.53	9.35

TABLE I: Number of events for data and MC backgrounds for the different tags in the full GSB; in the 2σ signal ellipse, the number of events selected in data and expected from the data sidebands; the number of data events selected inside the $\pm 2\sigma$ band in ΔE ; and the respective efficiencies (ε).

efficiency, tracking and photon reconstruction efficiencies, and particle identification are estimated to be 1.2%, 1.3%, 1.8% and 1.2%, respectively. We obtain a measure of the systematic error of the efficiency due to simulation uncertainties of the NN input variables by fixing each input variable to its average value one at a time, without retraining or changing the architecture of the NN, and re-calculating the efficiency. This has the effect of removing each input variable completely from the NN selection and gives a 1.9% relative error on the signal efficiency. Adding these errors in quadrature gives 3.4%. As we use 1.2×10^6 MC signal events, the contribution to the error arising from signal MC statistics is negligible.

Alternatively, these (and other potential sources of systematic uncertainty not necessarily accounted for in the above procedure) can be collectively estimated from the

detector modelling uncertainty obtained by comparing data to the MC backgrounds in the non-blinded part of the GSB, where the background and signal have similar properties apart from m_{EC} and ΔE . Data and MC background statistics as well as signal efficiencies (ε) are shown in Table I inside the full GSB. The agreement in the GSB between data and the background MC for each tag-mode and their combination validates the ability of the MC to simulate these signal-like events. The statistical precision of this data-to-MC ratio is augmented by using the expanded range $m_{EC} \in [1.0, 2.5] \text{ GeV}/c^2$ to obtain a value of $1.052 \pm 0.056(\text{stat}) \pm 0.024(\text{norm})$ in the non-blinded part of the GSB. To be conservative, we quote the total 6.1% uncertainty on this ratio, which includes a 2.3% normalization error on the product $L\sigma_{\tau\tau}$, as the relative systematic error on the ε in the GSB.

To obtain the branching ratio, we perform an extended unbinned maximum likelihood (EML) fit to the m_{EC} data distribution (Figure 2) after all requirements but that on m_{EC} have been applied. Within this $\pm 2\sigma$ band in ΔE the efficiencies for the different tag-modes are given in Table I for a total value of $\varepsilon = (9.4 \pm 0.6)\%$, where the systematic error here includes an additional contribution from the ΔE requirement. A linear parameterization describes the background and a double Gaussian serves as the probability density function (PDF) of the signal. Uncertainties in the mean and resolution of m_{EC} are incorporated into the fit by convoluting the signal PDF with another Gaussian with $\sigma = 4 \text{ MeV}/c^2$ and by increasing the σ of the convoluted Gaussian by $1 \text{ MeV}/c^2$. The quoted limit is insensitive to these variations, however.

In the EML fit, the number of signal events is given by $2L\sigma_{\tau\tau}\varepsilon\mathcal{B}(\tau^\pm \rightarrow \mu^\pm\gamma)$ and we fit for the branching ratio, the number of background events and slope of the background. The systematic uncertainty on ε is incorporated into the likelihood by adding ε as a fourth fit parameter under the constraint that it follows a Gaussian spread about its measured value within the estimated errors. This yields the same upper limit as the fit without the constraint on ε to within the quoted number of significant figures. The fit gives $\mathcal{B}(\tau^\pm \rightarrow \mu^\pm\gamma) = (-5.6^{+8.3}_{-6.3}) \times 10^{-8}$, which corresponds to $-2.2^{+3.2}_{-2.4}$ signal and 143 ± 12 background events. From the likelihood function of this fit, a Bayesian upper limit can be derived [18].

In keeping with established $\tau^\pm \rightarrow \mu^\pm\gamma$ studies [6, 19], we derive a frequentist upper limit [20]. We generate MC samples with Poisson-distributed numbers of signal and background events. The expected number of background events is fixed to 143 and we scan over the expected number of signal events, s . The m_{EC} values are distributed according to the signal and background PDFs, where the background slope is generated from a Gaussian distribution with mean and standard deviation given by the fit to the data. The number of signal events in each sample is extracted using the same EML fit procedure as that applied to the data. We vary s until we find a value for

which 90% of the sample yields a fitted number of signal events greater than that observed in the data, *i.e.* -2.2 . At 90% c.l. this procedure gives an upper limit of $\mathcal{B}(\tau^\pm \rightarrow \mu^\pm \gamma) < 6.8 \times 10^{-8}$ [21].

As confirmation of this result, we also undertake an analysis without the NN, having the same sensitivity of 12×10^{-8} for the expected 90% c.l. upper limit. Events with a tag-side muon are vetoed but single-track tag events are otherwise not classified. Cuts are applied on the signal μ momentum, signal γ energy, θ_{miss} , p_{miss}^T , the tag-side invariant mass and ΔE , and m_{EC} is required to be within 30 MeV of m_τ . This selection retains 10.7% of the signal and has a background of 28.5 ± 2.3 events as estimated from the sidebands.

To enhance the signal/background discrimination, a likelihood-ratio variable, \mathcal{R} , is built from four discriminating variables: p_{miss}^T , ΔE , the difference between the signal μ and γ energy in the c.m., and the acoplanarity between the signal $\mu\gamma$ system and the tag system. We observe no evidence of signal and we compare the two-dimensional (m_{EC} , \mathcal{R}) distribution of the 27 events in data with the background and signal expectations, utilizing a classical frequentist CL_{S+B} method [22]. The limit set is consistent with the above value and amounts to a 90% c.l. limit of 9.4×10^{-8} .

We are grateful for the excellent luminosity and machine conditions provided by our PEP-II colleagues, and for the substantial dedicated effort from the computing organizations that support *BABAR*. The collaborating institutions wish to thank SLAC for its support and kind hospitality. This work is supported by DOE and NSF (USA), NSERC (Canada), IHEP (China), CEA and CNRS-IN2P3 (France), BMBF and DFG (Germany), INFN (Italy), FOM (The Netherlands), NFR (Norway), MIST (Russia), and PPARC (United Kingdom). Individuals have received support from the A. P. Sloan Foundation, Research Corporation, and Alexander von Humboldt Foundation.

-
- [3] M. L. Brooks *et al.* [MEGA Collab.], Phys. Rev. Lett. **83**, 1521 (1999). This currently provides the most stringent limit of $\mathcal{B}(\mu^\pm \rightarrow e^\pm \gamma) < 1.2 \times 10^{-11}$ at 90% c.l.
 - [4] Y. Fukuda *et al.* [Super-Kamiokande Collab.], Phys. Rev. Lett. **81**, 1562 (1998); Q. R. Ahmad *et al.* [SNO Collab.], Phys. Rev. Lett. **89**, 011301 (2002); M. H. Ahn *et al.* [K2K Collab.], Phys. Rev. Lett. **90**, 041801 (2003); K. Eguchi *et al.* [KamLAND Collab.], Phys. Rev. Lett. **90**, 021802 (2003).
 - [5] B. W. Lee and R. E. Shrock, Phys. Rev. D **16**, 1444 (1977). A value of $\Delta m_{32}^2 \approx 3 \times 10^{-3} (\text{eV}/c^2)^2$ [4] and maximal mixing implies $\mathcal{B}(\tau^\pm \rightarrow \mu^\pm \gamma) \approx \mathcal{O}(10^{-54})$.
 - [6] K. Abe *et al.* [Belle Collab.], Phys. Rev. Lett. **92**, 171802 (2004).
 - [7] B. F. Ward, S. Jadach, and Z. Was, Nucl. Phys. Proc. Suppl. **116**, 73 (2003).
 - [8] *BABAR* Collab., B. Aubert *et al.*, Nucl. Instr. Meth. A **479**, 1 (2002).
 - [9] J. Z. Bai *et al.* [BES Collab.], Phys. Rev. D **53**, 20 (1996).
 - [10] Although the signal MC has been modelled using a phase space model, the limit obtained in this analysis is insensitive to this assumption as demonstrated by considering the two extreme cases of a V-A and a V+A form of interaction for the signal MC. The insensitivity is largely a consequence of the symmetric cut on $|\cos \theta_H|$.
 - [11] Particle Data Group, K. Hagiwara *et al.*, Phys. Rev. D **66**, 010001 (2002).
 - [12] S. Jadach, Z. Was, R. Decker, and J. H. Kuhn, Comp. Phys. Comm. **76**, 361 (1993).
 - [13] E. Barberio and Z. Was, Comp. Phys. Comm. **79**, 291 (1994).
 - [14] S. Agostinelli *et al.* [GEANT4 Collab.], Nucl. Instr. Meth. A **506**, 250 (2003).
 - [15] D. J. Lange, Nucl. Instr. Meth. A **462**, 152 (2001).
 - [16] T. Sjöstrand, Comp. Phys. Comm. **82**, 74 (1994).
 - [17] S. Brandt *et al.*, Phys. Lett. **12** (1964) 57; E. Fahri, Phys. Rev. Lett. **39** (1977) 1587.
 - [18] A Bayesian upper limit assuming a uniform prior can be obtained by integrating the likelihood function of the fit, L , from zero to the value of the branching ratio that includes 90% of $\int_0^\infty L(\mathcal{B})d\mathcal{B}$. This gives a 90% c.l. upper limit of $\mathcal{B}(\tau^\pm \rightarrow \mu^\pm \gamma) < 14 \times 10^{-8}$. Integrating from $-\infty$ instead of zero changes this to 7.9×10^{-8} .
 - [19] S. Ahmed *et al.* [CLEO Collab.], Phys. Rev. D **61**, 071101 (2000).
 - [20] I. Narsky, Nucl. Instr. Meth. A **450**, 444 (2000). Subsequent to this publication, its author recommended employing a fit convention that allows for a negative yield.
 - [21] For an equivalent experiment with no signal, the probability of obtaining a 90% c.l. upper limit at or below 6.8×10^{-8} is 30%.
 - [22] T. Junk, Nucl. Instr. Meth. A **434**, 435 (1999); A. L. Read, J. Phys. G: Nucl. Part. Phys. **28**, 2693 (2002).

* Also with Università della Basilicata, Potenza, Italy

† Deceased

- [1] J. Hisano and D. Nomura, Phys. Rev. D **59**, 116005 (1999).
- [2] S. F. King and M. Oliveira, Phys. Rev. D **60**, 035003 (1999).